NI

NASA Technical Memorandum 82811

Tungsten Fiber Reinforced Superalloy Composite High Temperature Component Design Considerations

Edward A. Winsa
Lewis Research Center
Cleveland, Ohio

Prepared for the
One-hundred-eleventh Annual Meeting of the American Institute of Mining, Metallurgical and Petroleum Engineers
Dallas, Texas, February 14-18, 1982

NASA

TUNGSTEN FIBER REINFORCED SUPERALLOY COMPOSITE HIGH TEMPERATURE COMPONENT DESIGN CONSIDERATIONS

Edward A. Winsa

National Aeronautics and Space Administration
Lewis Research Center
Cleveland, Ohio 44135

SUMMARY

Tungsten fiber reinforced superalloy composites (TFRS) are intended for use in high temperature turbine components. Current turbine component design methodology is based on applying the experience, sometimes semi-empirical, gained from over 30 years of superalloy component design. Current composite component design capability is generally limited to the methodology for low temperature resin matrix composites. Often the tendency is to treat TFRS as just another superalloy or low temperature composite. However, TFRS behavior is significantly different than that of superalloys, and the high temperature environment adds considerations not common in low temperature composite component design. This paper describes the methodology used for preliminary design of TFRS components. Considerations unique to TFRS are emphasized.

Introduction

Tungsten Fiber Reinforced Superalloy composites (TFRS) offer an alternative to monolithic superalloys when designing components for demanding high temperature applications. These members of the Fiber Reinforced Superalloy composite (FRS) family have exhibited use temperature potential up to 150 K greater than the best superalloys (Ref. 1). Moreover, cost effective fabrication feasibility has been demonstrated (Figs. 1 and 2, Refs. 2 and 3).

Despite their promise, TFRS will remain laboratory curiosities until rig or engine tests can confirm their utility in actual components. Recognising this fact, NASA contracted with the General Electric Co. - Aircraft Engine Group (Evandale, Ohio) to conduct a "Hardware Designers' Overview of Tungsten-Fiber Reinforced Superalloy Composites for Turbojet Engines". One objective of the "...Overview..." was to select three potentially practical TFRS engine components and develop preliminary designs using a first generation TFRS (W/FeCrAlY, Ref. 4). The most promising component could then be detail designed, fabricated, and rig tested in a possible following sequence of programs and contracts. Preliminary designs for a turbine blade, turbine vane, and an outlet guide vane (OGV) resulted from the contract.

Designing the "...Overview..." contract components necessitated a joint effort by General Electric (GE) and NASA (Fig. 3). GE and NASA collaborated to select engine components and establish the geometry and property requirements of the TFRS versions. Next, NASA determined the TFRS laminate configuration needed to meet the requirements and calculated the appropriate physical and mechanical properties. Then, GE used the calculated laminate properties in performing a structural and heat transfer analysis of the components. Because these were preliminary "screening" designs, no optimization of the components was attempted.

This report briefly reviews the major considerations and methodology used by NASA to design the TFRS laminated airfoils used in the three components. Emphasis is placed on those considerations which make TFRS components somewhat unique relative to superalloy or low temperature composite components.

TFRS Airfoil Design Considerations

TFRS was used in only the airfoils of the blade, vane, and OGV preliminary designs. This section indicates some of the considerations that affect TFRS airfoil design.

Film cooling is currently the most efficient proven superalloy airfoil cooling technique. It has been used successfully for turbine blades and vanes. However, its utility with TFRS is questionable. The reason being that film cooling holes would probably have to cut through tungsten reinforcing fibers, and that could cause two problems. First, the TFRS airfoil would be weakened because discontinuous fibers provide less reinforcement.

Second, unless the holes were subsequently coated, the airfoil's susceptability to oxidation damage would increase. Although these are not necessarily insurmountable problems, it would be best to avoid them by avoiding film cooling, if possible.

TFRS may be convection cooled and impingement cooled with or without a Thermal Barrier Coating (TBC). In fact, a TFRS airfoil with impingement cooling plus a TBC might be an attractive combination of technologies (Fig. 4). Previous calculations indicated that Impingement/TBC (ITBC) cooled TFRS airfoils could theoretically operate in near stoichiometric temperature inlet gas streams (Ref. 5). Furthermore, the tailorability of TFRS thermal expansion could allow increased durability of TBC on TFRS relative to its durability on superalloys. Moreover, ITBC cooled TFRS airfoils without film cooling holes should exhibit greater aerodynamic efficiency and lower LCF (low cycle fatigue) stresses than film cooled airfoils. The greater aerodynamic efficiency would be due to the lack of undesirable air turbulance normally associated with air jetting out of film cooling holes. The lower LCF stresses would be due to the lack of stress concentrations caused by film cooling holes cutting through the airfoil wall. Finally, as will be indicated below, ITBC cooled TFRS may have the same cooling efficiency as film cooled superalloys.

Only moderately complex internal geometries may be feasible with hollow TFRS airfoils. The TFRS fabrication process indicated in figure 5 utilizes a leachable steel core to provide the hollow cavity (Ref. 2). This approach permits the easy incorporation of trailing edge cooling holes and simple ribs. However, complex serpentine rib schemes could be difficult to achieve.

The leading edge of hollow TFRS airfoils must be of wrap around construction. The exact construction shown in figure 5 leads to a seam at the leading edge of the airfoil (Fig. 1). Calculations indicate that failure could occur at the seam of hollow airfoils (not a problem with solid airfoils). Thus the plys must wrap around the leading edge of hollow airfoils to eliminate the seam. The feasibility of the wrap around technique has been demonstrated for the blade shown in Fig. 1 (Ref. 2).

The allowable tungsten fiber diameter is limited by several conflicting considerations. Fiber reaction (see below) requires that the largest possible fiber diameter be used. On the other hand, the minimal thickness of hollow airfoil walls combines with the need for laminate symmetry (i.e., several plys must be used) to keep allowable diameters small. Using a weak matrix (e.g., FeCrAlY) has the same effect because smaller diameter fibers are needed to decrease fiber critical length and, thereby, increase reinforcement efficiency (Ref. 6). Yet, if impact strength is needed, larger diameters should be used (Ref. 7). Typically, allowable fiber diameters range between 0.1mm and 0.2mm; although, for larger components, diameters up to 0.4mm are useful.

Special attachment schemes must be developed for TFRS blades and vanes. Blade dovetail and vane bands will probably have to be made from superalloys to save weight and provide maximum strength at the component/engine inter-

face. However, the low thermal expansion of TFRS laminates could cause problems if simple brazed or diffusion bonded attachments were used. The attachment problem is being addressed by NASA research.

Use of TFRS blades as substitutes for currently used turbine blades will probably be seriously hampered by disc size and strength limitations. Current discs are optimised for superalloy blades. Typically, there is no extra physical space around the disc to allow its enlargement to accomodate slightly heavier TFRS blades.

Turbine Material Property Considerations

TFRS properties cannot be directly compared to superalloy properties. Current turbine material requirements were established during over three decades of design/use experience with monolithic superalloys (Table I). There is no similar history of experience with TFRS. Consequently, there is a natural tendency to use superalloy requirements when evaluating TFRS properties. However, this practice can result in misleading evaluations. For example, TFRS seem to have inferior LCF capability relative to the best superalloys (appendix A and Ref. 8). But, in fact, the modulii, thermal conductivity, and thermal expansion properties of TFRS drastically reduce LCF stresses caused by thermal gradients (see below). Thus, TFRS may actually outperform the best superalloys in some applications where LCF is the limiting failure mode. Therefore, the suitabilty of TFRS for specific applications must be determined by design and analysis using composite theory - not by direct comparison between TFRS and superalloy properties.

Material properties must be well characterized to allow detailed component design and analysis. Table II indicates the minimum property characterization generally desired for initial design consideration of superalloys.

Unfortunately, TFRS properties cannot be easily summarized as can superalloy properties. The reason being that TFRS are laminated structures, not simple materials. Literally thousands of valid permutations of fiber diameter, volume percent, and fiber angle versus ply sequence exist for even simple TFRS laminated structures. The overwhelming quantity of variations makes thorough characterization of each variation impossible. Moreover, the properties of TFRS laminates are highly geometry dependent; for example, merely changing the width of an angle plied test panel can drastically affect the strength properties. Therefore, unlike the situation for superalloys, tests conducted on simple TFRS laboratory specimens can give grossly misleading indications of component performance. Consequently, TFRS components must be designed and analyzed using composite theory; then, the TFRS laminates determined by the design process must be tested in a form as close to their component geometry as possible.

The TFRS laminate must be custom designed for each specific component application. Such custom design is not always required for the better known low temperature composites (e.g., Graphite/Epoxy, Boron/Aluminum). The reason is that components made of such better known composites tend to be very large relative to the fiber critical length; therefore, critical length is not a factor. Furthermore, their reinforcing fibers have low density

which makes maximum volume percent reinforcment practical. Also, fiber reaction degradation during service is usually not a factor. Consequently, standard panels of these composites can be characterized and the resulting properties used for design (e.g., $\pm 15^{\circ}$, 50 volume percent, 0.2mm diameter Boron fiber, 1100 Aluminum matrix B/Al for fan blade airfoils). By comparison, the small size of typical TFRS airfoils combined with the density and reaction degradation of tungsten fibers require that all TFRS laminate parameters be optimized.

Ideally, when designing TFRS components, one would like to have the capability to completly determine the component properties and performance using only fiber and matrix properties combined with composite theory (Fig. 6). Essentially, that is what was attempted in the NASA design of the "... Overview..." laminates. But the methods used are still under developement; thus, significant errors were possible. Hence, conservatism and safety factors were employed to increase the probability of successful design.

TFRS Laminate Analysis Considerations

The NASA approach used to analyze the TFRS laminates used for the GE components is flow diagramed in figure 7. The rest of this section is an overview of principal considerations relevant to the TFRS laminate analysis methodology of figure 7. Some typical calculated laminate properties for W - 1.5ThO_2/FeCrAlY are given in the Appendix.

Fiber Degradation

Fiber degradation in the forms of diffusion induced recrystallization and partial dissolution is a chief cause of TFRS property degradation. The appearance of recrystallized fibers is illustrated in Fig. 8. The reaction penetration depth (P) is defined as the distance measured from the location of the original perimeter of the unreacted fiber to the perimeter of the unreacted core of the fiber.

Reaction penetration depth is adequately defined by the following equation.

$$P = (Po^2 + D \exp(-G/T)\ t)^{1/2}$$

where:

Po initial reaction penetration depth due to the TFRS laminate fabrication process

D a curve fitting parameter

G a curve fitting parameter

T temperature (absolute)

t time of exposure to temperature

This equation allows extrapolation of limited data to any temperature/time condition. But, because the equation is approximate, final designs must be based on reaction data acquired at the temperature/time of interest.

TFRS tensile, stress-rupture, and LCF property calculations were based on the conservative assumption that the properties of the fiber reacted zone were those of the matrix. In effect, this conservative assumption amounted to reducing the actual fiber content to a pseudo fiber content. The ratio of the pseudo content/actual content equals the ratio of unreacted core area/original fiber area.

Actual components usually have a complex temperature/time history. For example, a turbine blade might see hot spots of 1150 K for a total of 7000 hr, 1250 K for 1000 hr, 1275 K for 700 hr, and 1325 K for 300 hr during a 9000 hr lifetime. We estimated the total reaction penetration using the following equation.

$$P = Po^2 + \int_0^t D \exp(-G/T)\, dt \,^{1/2}$$

To be conservative, we assumed that the total reaction penetration (P) was present at the first instant of component operation.

Tensile Properties

TFRS laminate tensile properties were estimated from fiber and matrix tensile properties combined with appropriate composite theory. The estimates were used for preliminary component design optimization. However, before attempting to produce components, the estimated properties would have to be verified by tests of TFRS laminated panels and component-like shapes.

Derivation of the laminate constitutive equations we used was predicated on the assumption that the plys could be treated as homogenious, anisotropic, elastic sheets. Their derivation and use has been reported by others (Ref. 9).

These linear equations were used to generate TFRS laminate elastic-plastic stress versus strain curves by a piecewise linear, step loading approach. The stresses on the plys, fibers and matrix were calculated at each step of the laminate loading process (Fig. 7).

Two useful relationships resulting from the laminate piecewise linear analysis were laminate stress versus strain diagrams and maximum fiber stress versus laminate stress diagrams (Figs. 9 and 10). The plots shown in the figures are for a simple longitudinal loading case at 1225 K. Similar diagrams were generated for a variety of complex loading cases wherein longitudinal, transverse, and shear loads were applied in the proportions expected in the TFRS component. Moreover, behavior over the range of important temperatures was calculated. The final laminate designs optimized the response to complex loads over the operational temperature spectrum. In addition to the stress relationships, laminate "elastic" constants were

generated for Stage I and Stage II deformation. These constants were used by GE during component analysis.

Laminate Failure Prediction

Tensile, stress-rupture, and LCF failure criteria were used to determine the suitability of laminates used in the blade, vane, and OGV. A range of loading patterns and temperatures were assessed for each component.

Tensile Failure. Tensile "failure" was assumed when laminate strain exceeded 1 percent (Fig. 9) or fiber-effective-stress (von Mises stress) exceeded the fiber-yield-stress in any ply (Fig. 10). Actual fracture would normally occur at over 5 percent elongation.

Stress-Rupture Failure. The laminate stress-rupture strength was defined by the stress rupture strength of the unreacted fiber cores. Laminate stress-rupture strength for a given lifetime was defined as that laminate stress which produced a maximum fiber-effective-stress (in the core) equal to the fiber stress-rupture strength for the same lifetime (Fig. 10).

LCF Failure. The laminate LCF strength versus cycles was defined by the LCF strength versus cycles behavior of the unreacted fiber cores. As with stress-rupture, the laminate LCF strength was defined as that laminate stress which produced a maximum fiber-effective-stress (in the core) equal to the LCF strength of the fibers (Fig. 10).

Miscellaneous Properties

The following miscellaneous physical properties were calculated by NASA for use by GE during TFRS component analysis.

Density and specific heat were both calculated as the weighted average of the fiber and matrix values (Rule of Mixtures).

Laminate thermal expansion coefficients were calculated during the previous laminate tensile analysis. The instantaineous expansion coefficients are a function of the TFRS laminate matrix stress state. Hence, they vary from, typically, 10 μm/m per °K during stage I to about 5.5 μm/m per °K during stage II elongation.

Individual ply conductivities were calculated with the methods of Ref. 10. Typical values are indicated in Fig. 11. To calculate laminate conductivities, the individual ply conductivities were combined in series or in parallel as required.

Components Considered in Design Overview

Three components received major attention during the GE TFRS design overview. As previously mentioned, these were a turbine blade, turbine vane, and an OGV. Only the key findings are alluded to below.

It is important to realize that all three components were designed and evaluated using W-1.5 ZrO_2/FeCrAlY. This is a moderate strength TFRS being used primarily as a model FRS system but which may also have practical utility (Ref. 4). Much stronger fibers (e.g., W-Re-Hf-C, Ref. 1) have been tested, and stronger matrixes are under development. Consequently, the findings indicated below do not reflect the ultimate potential of TFRS.

Turbine Blade

An advanced Stage 1 turbine blade was redesigned and analyzed as a paper experiment to evaluate cooling techniques. The current superalloy blade operates at relatively high stress/low temperature; whereas, W/FeCrAlY is better suited to moderate stress/high temperature applications. Thus, in this analysis W/FeCrAlY performance was expected to be less desirable than the superlloy performance. Nonetheless, GE's design experience with this blade made it ideal as a vehicle to evaluate the efficency of ITBC cooling versus film cooling.

GE found that an ITBC cooled blade was the best design approach for TFRS, as expected (Fig. 12). TFRS film cooled and impingement cooled (without TBC) designs were also evaluated. The cooling efficiency of an ITBC cooled TFRS blade (0.190 mm TBC) equaled that of the advanced film cooled blade. However, the TFRS blade provided no significant use temperature advantage, as expected.

We infer from the NASA/GE results that a TFRS ITBC blade using stronger W-Re-Hf-C fibers could have significant potential. Aerodynamic efficiency should be higher than possible with film cooled superalloy blades. Moreover, the lack of cooling hole stress concentrations and the reduced temperature gradients due to high TFRS conductivity and the TBC might result in improved LCF capability (relative to superalloy blades). However, the target engine would have to be specifically designed to make optimum use of TFRS blades.

Turbine Vane

A convection cooled vane was evaluated because it was considered to be an ideal application of current moderate strength TFRS technology (Fig. 13). The geometrically simple, convection cooled (no TBC) airfoil could be fabricated using previously developed techniques (Ref. 2). And the improved temperature capability of TFRS should permit reduced coolant flow for greater engine efficiency.

Stresses in the TFRS vane were substantially lower than in a comparable superalloy vane according to GE calculations. The lower stresses derived from the fact that the TFRS laminate had lower thermal expansion, lower modulus, and higher conductivity than commonly used cobalt-base superalloys. This combination reduced thermal stresses which are the chief source of stress in the vane.

Further evaluation at NASA suggests that a TFRS ITBC Stage 1 vane is potentially very attractive. ITBC cooling could provide the efficiency of currently used film cooling without the associated aerodynamic penalty.

Furthermore, cooling hole stress concentrations would be absent, and the TBC would lower temperature gradients in the TFRS. Those benefits combined with the inherently low thermal stresses in TFRS could significantly reduce TFRS vane susceptability to LCF failure (relative to superalloy vanes). Since LCF is a principal failure mode in Stage I vanes, the reduced LCF susceptibilty of TFRS would be highly advantageous.

Outlet Guide Vane

A TFRS OGV was considered because it offered a low risk application. Moreover, the relatively simple solid OGV airfoil was felt to be a good first candidate for rig tests (Fig. 14). The NASA/GE results indicate that a TFRS OGV may exhibit much longer life than a superalloy OGV.

Concluding Remarks

TFRS has promise as an airfoil material in advanced aircraft turbines. The aerodynamic and cooling efficiencies of an ITBC cooled TFRS airfoil could exceed those of film cooled superalloy airfoils. Thermal stresses, which are a leading cause of failure in some applications, could be inherently lower in TFRS airfoils because TFRS has lower thermal expansion, lower modulii, and higher conductivity than most superalloys. Moreover, even moderate strength TFRS (W-1.5 ThO_2/FeCrAlY) seems adequately strong for some turbine vane and outlet guide vane applications.

None the less, more development and understanding is needed before TFRS will be ready for engine testing. For example, airfoil-to-engine attachment schemes must be developed and demonstrated. Stronger fibers (e.g., W-Re-Hf-C) must be developed to make TFRS blades more attractive. Component rig test experience must be acquired. And a larger TFRS laboratory specimen data base must be developed to expedite refinement of TFRS computational structural analysis and design methodologies. Current NASA programs are addressing these needs.

APPENDIX

Calculated TFRS Vane Airfoil Material Properties After Long Term Exposure to Vane Conditions Using Moderate Strength Tungsten Fibers

A. TFRS Composition

Fiber > W - 1.5 ThO_2 Matrix > Fe - 24 Cr - 6 Al - 1 Y
Average fiber volume fraction > 0.59
Density > 14000 kg/m^3

B. Thermal Properties

Thermal conductivity

Temp.	Span and chord	Through wall
920 K	56 W/mK	45 W/mK
1310 K	57 W/mk	52 W/mK

Thermal expansion (typical)
9.1 μm/m during Stage I elongation
7.5 μm/m during Stage II elongation

C. Mechanical Properties

Tensile properties at 1255 K
(Same in span and chord directions, semi-isotropic)

Ultimate strength 235 MPa
Ultimate elongation > 5 percent

Property	Stage I elongation	Stage II elongation
Elastic mod.	210 GPa	52 GPa
Shear mod.	81 GPa	19 GPa
Poisson's rat.	0.301	0.334
Yield stress	21 MPa	165 MPa
Yield strain	98 μm/m	2700 μm/m

Low cycle fatigue (LCF) for 36000 cycles
(Same in span and chord directions)

Temp.	Alternating stress range
1255 K	185 MPa
1365 K	165 MPa

Stress-rupture at 1310 K for 500 hr = 145 MPa

References

1. D. W. Petrasek and R. A. Signorelli: NASA TM 82590, 1981.

2. P. Melnyk and J. N. Fleck: Report No. TRW-ER-8101, TRW, Inc., Cleveland, O., Dec. 1979 (NASA CR-159788).

3. C. F. Barth, D. W. Blake and T. S. Stelson: Report No. TRW-1ER-7930, TRW, Inc., Cleveland, O., Oct. 1977 (NASA CR-135203).

4. D. W. Petrasek, E. A. Winsa, L. J. Westfall and R. A. Signorelli: NASA TM-79094, 1979.

5. E. A. Winsa, L. J. Westfall, and D. W. Petrasek: NASA TM-73842, 1978.

6. R. W. Jech: NASA TN D-5735, 1970

7. E. A. Winsa and D. W. Petrasek: NASA TN D-7393, 1973.

8. G. I. Friedman and J. N. Fleck: Report No. TRW-ER-8135, TRW, Inc., Cleveland, O., Oct. 1979 (NASA CR-159720).

9. J. E. Ashton, J. C. Halpin and P. H. Petit: Primer on Composite Materials Analysis. Progress in Materials Science Series, Vol. 3, Technomic Publishing Co., Inc., Westport, Conn., 1969.

10. L. J. Westfall and E. A. Winsa: NASA TP 1445, 1979.

Table I. - Material Characteristics Important in Turbine Blade Applications

Property	Significance to Design
Creep and rupture	Limit allowable airfoil metal temperature and stress
High cycle fatigue	Vibration stresses at all locations on the blade must be less than the endurance limit of the material, as determined in smooth and notched bar tests
Low cycle fatigue	Determines design, life: smooth bar data important to airfoil leading and training edges; notched bar data important to dovetail and bleed holes in air cooled blades
Tensile	Limits dovetail/shank design
Combined steady state and vibratory	Vibratory stress endurance limit is reduced by presence of steady state stresses
Shear and torsion	Adequate in conventional superalloys, but could be limiting in anisotropic materials, particularly in the dovetail
Density	Affects blade and disk stresses
Thermal expansion	Affects blade expansion, important to gas leakage and tip rub
Incipient melting	Affects over-temperature capability of airfoil in the event of hot spots
Elastic constants	Affect blade material frequencies, and thermal stresses

Table II. - Minimum Property Data Needed to Design Turbine Blades for Development Engines

Property	Temperature or temperature range, °K						
	RT	775	900	1025	1150	1275	1400
0.2 percent	X	X	X	X	X	X	X
UTS	X	X	X	X	X	X	X
Percent El.	X	X	X	X	X	X	X
R of A	X	X	X	X	X	X	X
100 hr SR				X	X	X	X
1000 hr SR				X	X	X	X
Plastic creep (0.2 percent)				X	X	X	X
Low cycle fatigue			X		X	X	X
High cycle fatigue			X		X	X	
Joint efficiency (if applicable)							
- UTS	X	X	X	X	X	X	X
- Percent El.	X	X	X	X	X	X	X
- 1000 hr SR			X		X	X	X
Stability-RT and 1150 K tensile ductibility, charpy and ballistic impact before and after 100 hr exposure to critical elevated temperatures	X				X		
Lowest melting temp.							
Density	X						
Thermal exp.		E S T I M A T E D					
Thermal cond.		E S T I M A T E D					
Spec. heat		E S T I M A T E D					
Poisson's ratio		E S T I M A T E D					
Mod. of elasticity	X	X	X	X	X	X	X

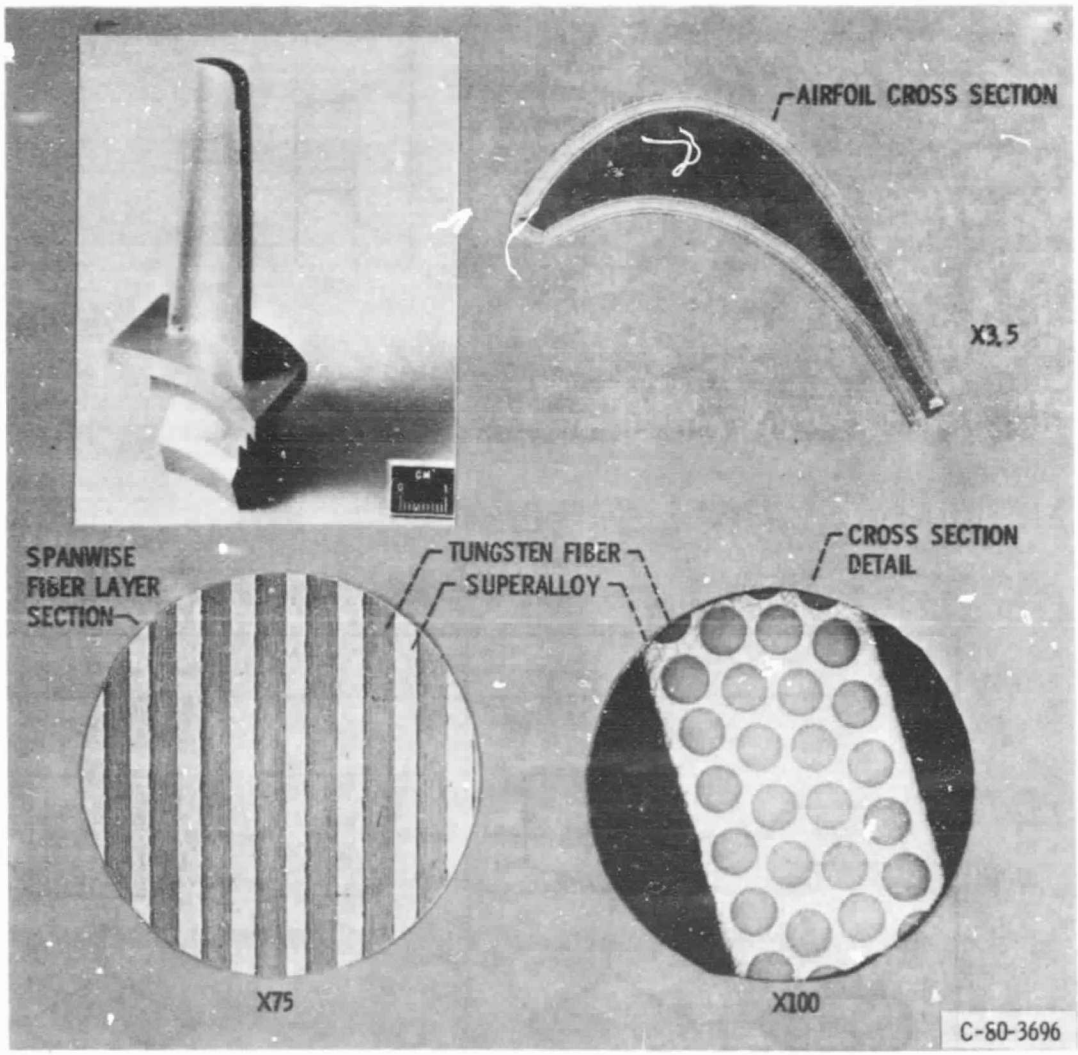

Figure 1. - TFRS blade fabrication was demonstrated using a convection cooled JT9D-like airfoil mated to a circular arc dovetail.

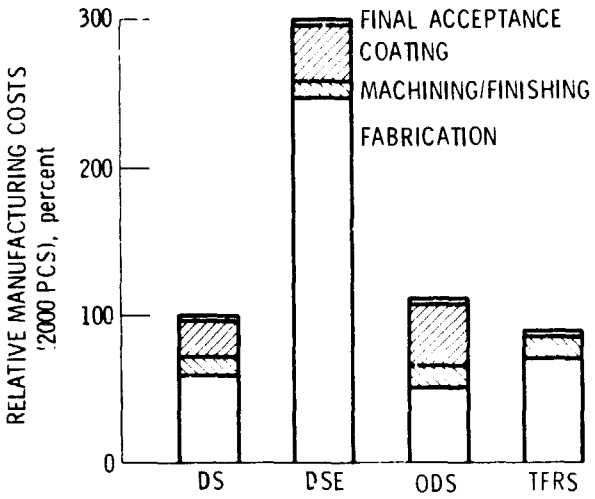

Figure 2. - TFRS fabrication costs are competitive with those of Directionally Solidified (DS) superalloys, DS Eutectics (DSE), and Oxide Dispersion Strengthened (ODS) Superalloys (Ref. 3).

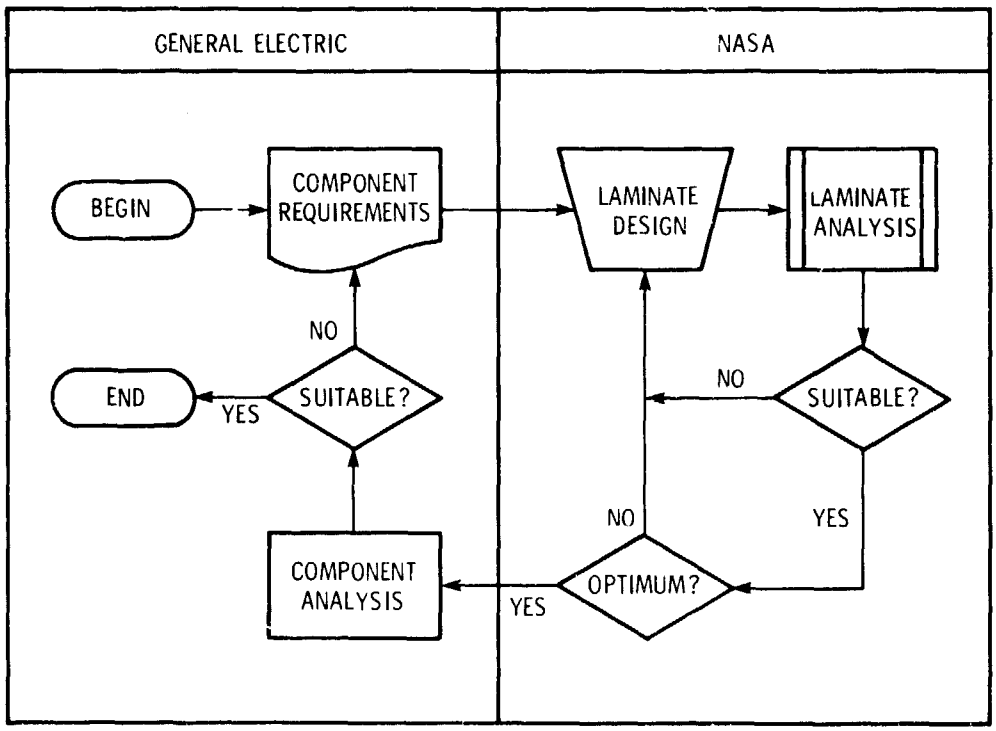

Figure 3. - "..Overview.." contract TFRS component design responsibility was shared by General Electric and NASA.

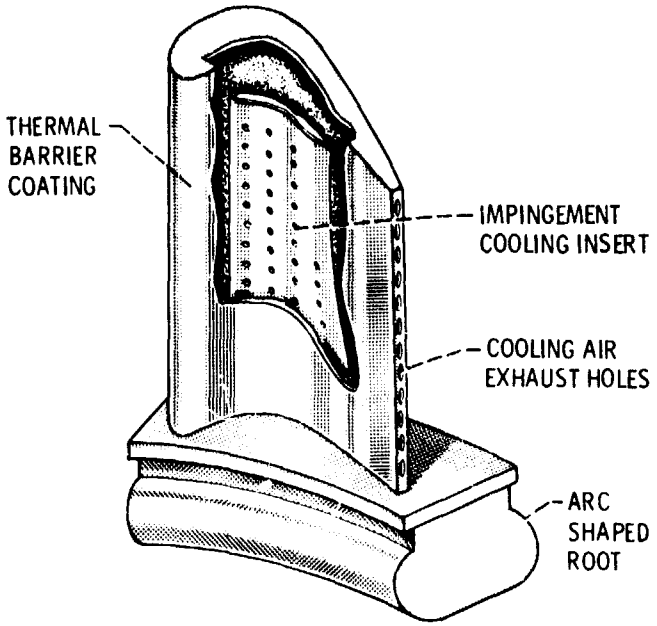

Figure 4. - Blade and Vane designs incorporating both impingement cooling and a Thermal Barrier Coating (TBC) may be optimum for TFRS.

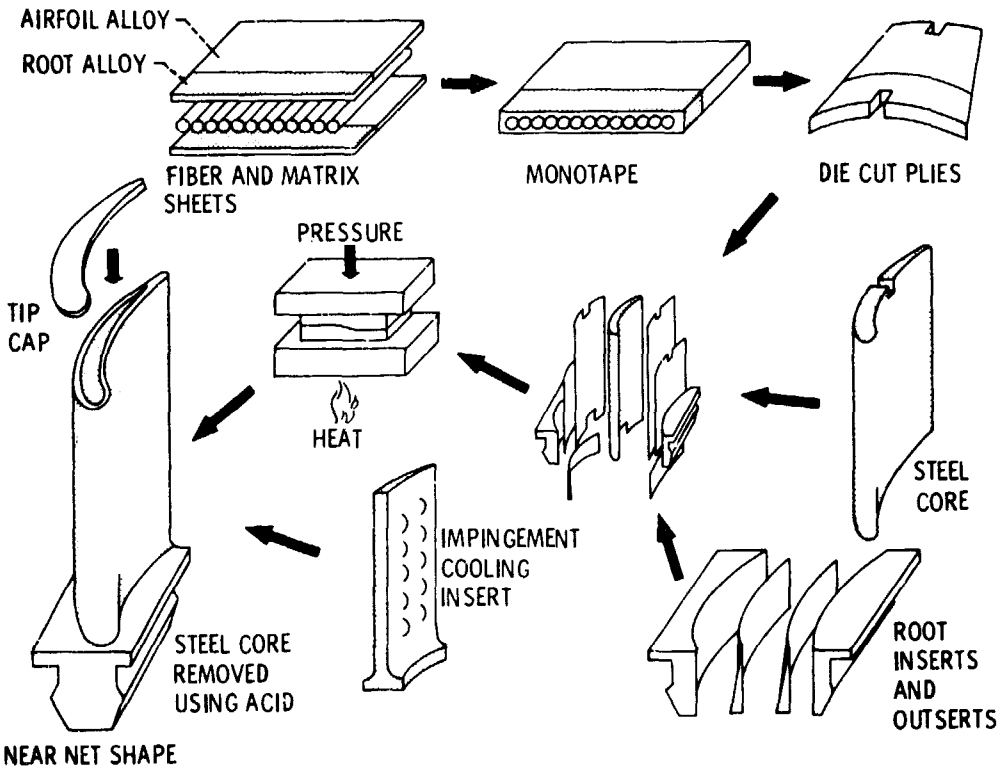

Figure 5. - The TFRS blade fabrication sequence is similar to that used for B/Al fan blades (note dual alloy plies) (Ref. 2).

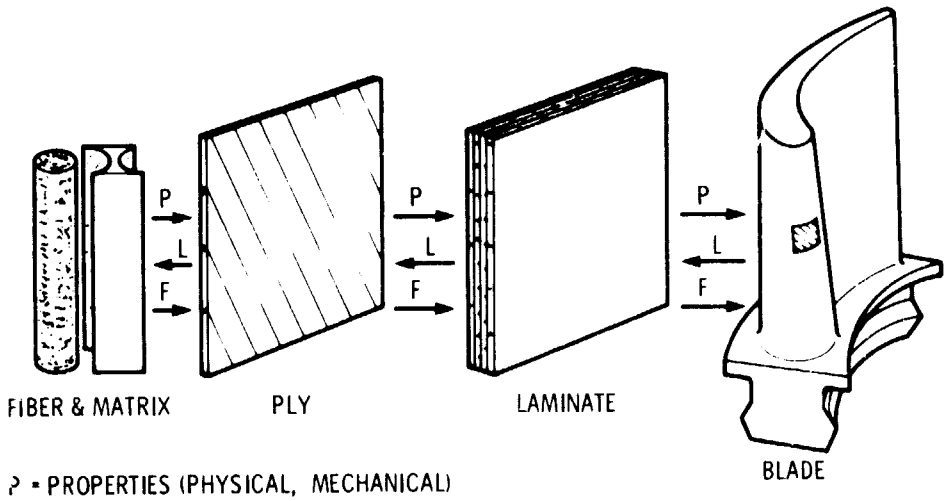

Figure 6. - Design of TFRS components requires the ability to predict component characteristics in terms of fiber and matrix characteristics.

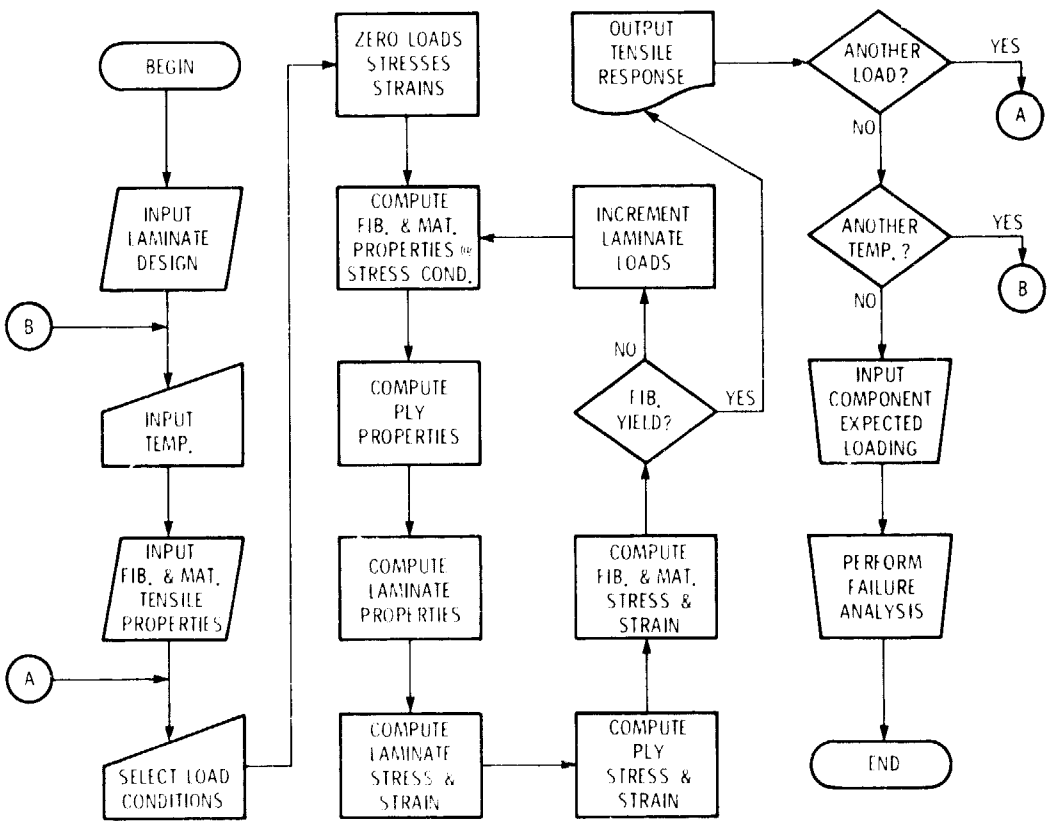

Figure 7. - TFRS laminate characteristics were computed for a range of load/temperature conditions using a piecewise linear approach to allow for plasticity.

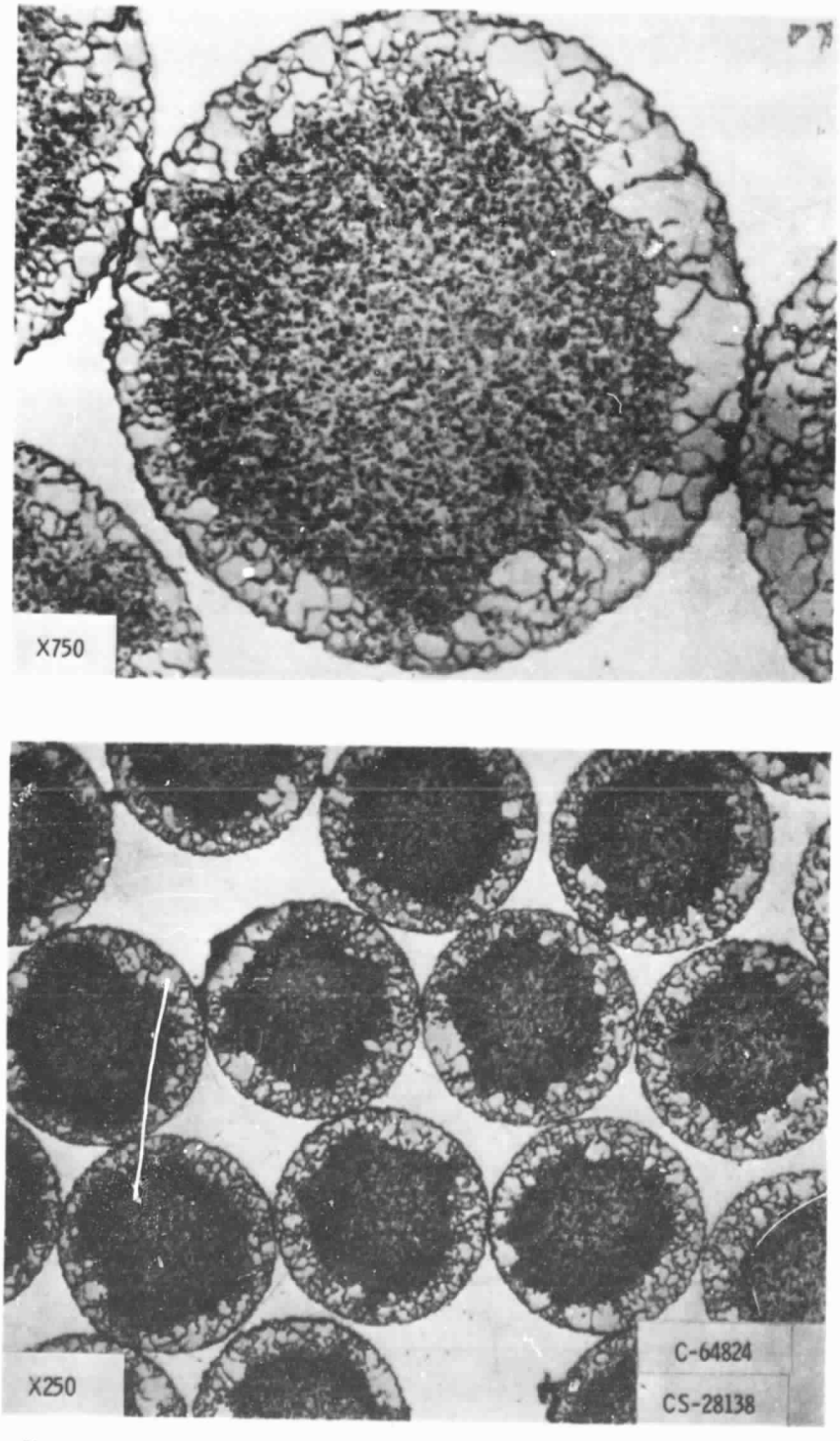

Figure 8. - Fiber recrystallization and dissolution due to elemental diffusion is the chief cause of TFRS property degradation with time.

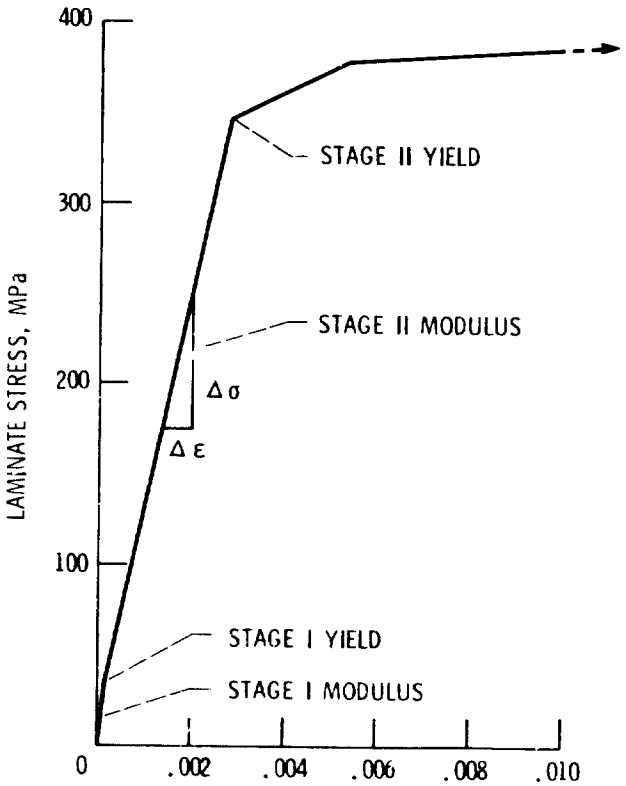

Figure 9. - Calculated TFRS laminate behavior is characterized by two stages of "elastic" deformation (W-1.5ThO2/FeCrAlY airfoil laminate in simple spanwise tension at 1225K).

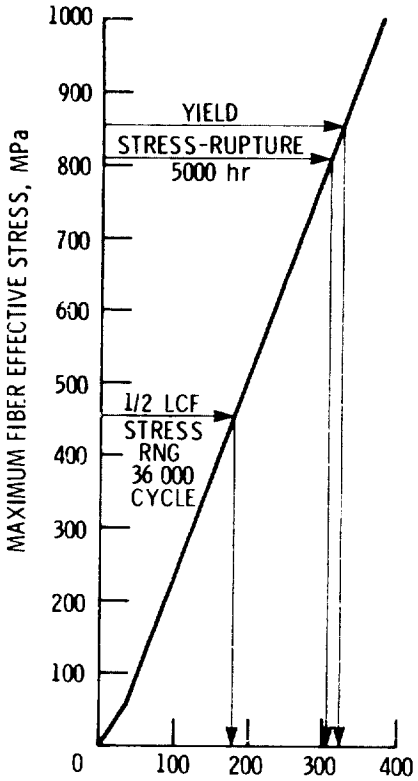

Figure 10. - Laminate Failure Calculation Approach. Since composite yield, stress-rupture, and LCF failure are fiber controlled, plots such as this one were used to predict laminate failure (plot for conditions of Figure 9).

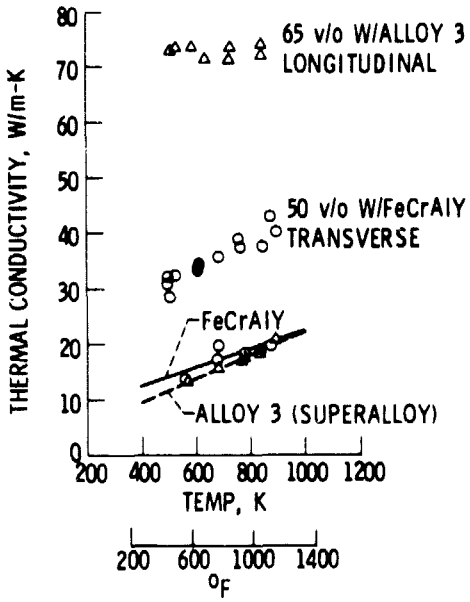

Figure 11. - TFRS conductivity is typically much higher than superalloy conductivity.

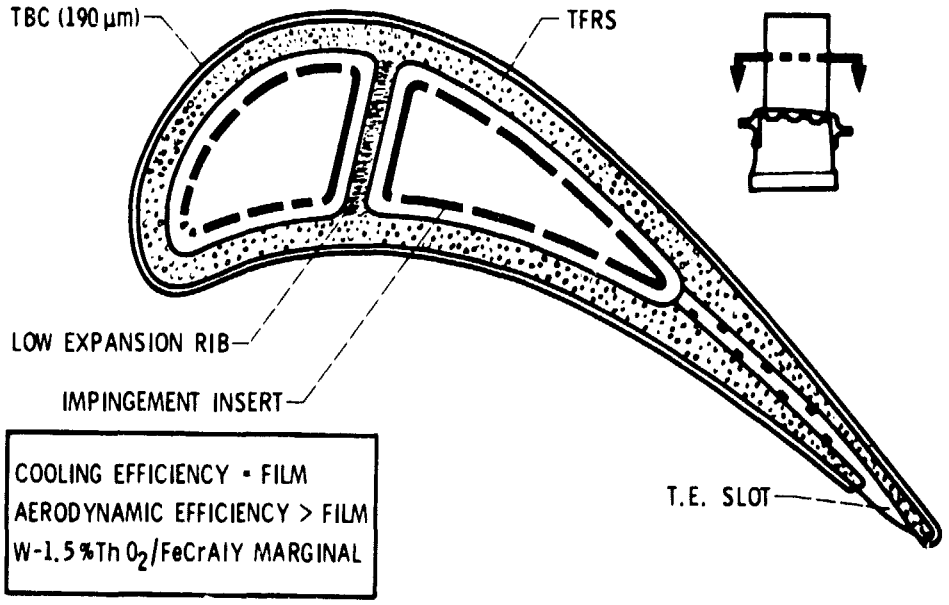

Figure 12. - TFRS blades of this general design could be viable if strong fibers (e.g., W-Re-Hf-C) were used.

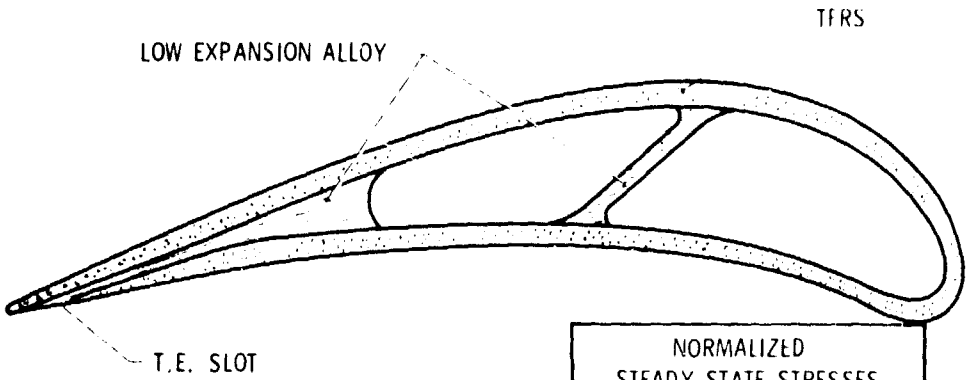

TFRS STRESSES LOW BECAUSE
TFRS α < SUPERALLOY α
TFRS k > SUPERALLOY k
TFRS E < SUPERALLOY E

	NORMALIZED STEADY STATE STRESSES	
	TFRS	SUPERALLOY
SPAN	0.15	1.00
CHORD	0.20	1.00
SHEAR	0.50	1.00

Figure 13. - TFRS convection cooled vanes should exhibit lower stresses than superalloy vanes because of substantial physical property differences.

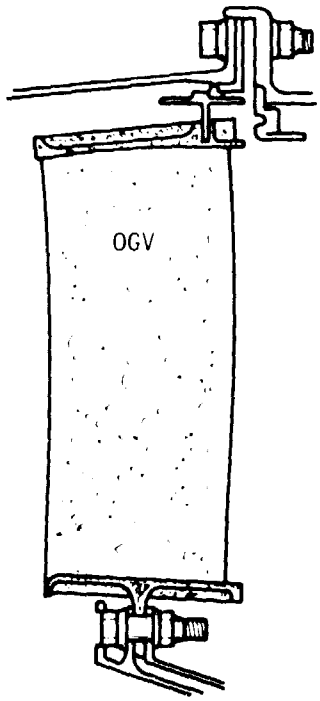

Figure 14. - A TFRS Outlet Guide Vane (OGV) could be used to gain design and rig test experience with first generation TFRS composites.